Search for individual UHECR sources in the future data

Gwenael Giacinti* **and Dmitri V. Semikoz***

**AstroParticle and Cosmology (APC), 10 rue Alice Domon et Léonie Duquet, 75205 Paris Cedex 13, France*

Abstract. **We propose a new way to detect individual bright Ultra-High Energy Cosmic Ray (UHECR) sources above background if the galactic magnetic field (GMF) gives the main contribution to UHECR deflection [1]. The method can be directly applied to maps given by experiments. It consists of starting from at least two high energy events above 6×10^{19}eV, and looking at lower energy tails. We test the efficiency of the method and investigate its dependance on different parameters. In case of detection, the source position and the local deflection power are reconstructed. Both reconstructions are strongly affected by the turbulent GMF. With the parameters adopted in this study, for 68% of reconstructed sources, angular position is less than one degree from real one. For typical turbulent field values of 4μG near the Earth, one can reconstruct deflection power with 25% precision in 68% of cases.**

Keywords**: ultra high energy cosmic rays, magnetic fields, Galaxy**

I. Introduction

The observation of the Greisen-Zatsepin-Kuzmin (GZK) cutoff [2] by HiRes experiment [3], followed by its confirmation by Pierre Auger Observatory [4] proves the astrophysical origin of UHECR. The UHECR sources are still unknown. Some possible candidates can be studied from the point of view of acceleration mechanisms -see refs. [5], [6], [7].

Their detection is difficult due to the UHECR deflections in the extragalactic and galactic magnetic fields. One can either wait for enough data at the highest energies to find a class of UHECR sources, or search for the first individual brightest sources. In this study, we investigate this last possibility.

We propose here a method to find UHECR sources on top of background and reconstruct their positions. We show that one has to start from at least two events with energies above $10^{19.8}$eV $\sim 6 \times 10^{19}$eV before looking at lower energy tails, in order to avoid confusion by background. We investigate the performance of this method depending on the different relevant parameters.

We assume as in [8] that UHECR deflections due to the extragalactic magnetic fields are negligible compared to the deflections due to the GMF. For an example of non negligible extragalactic contributions, see [9]. The GMF is divided in two components (regular and turbulent). For the regular one, we take the Prouza and Smida model [10], [11]. It consists of a thick disk, with a halo and a dipole field. Following latest knowledge on the GMF [12], [13], we modified some parameters and took an exponentially decaying profile along the galactocentric radius. The field value close to the Sun is B_{reg} = 1-3μG (currently admitted value: B_{reg} = 2μG). The model for the turbulent component is described in [1]. The RMS value of the turbulent field decays as 1/r along the galactocentric radius r, and exponentially along the direction orthogonal to the galactic plane. The plane thickness is set to 1.5 kpc. The turbulent field value close to the Sun is B_{turb} = 2-8μG (currently admitted value: B_{turb} = 4μG).

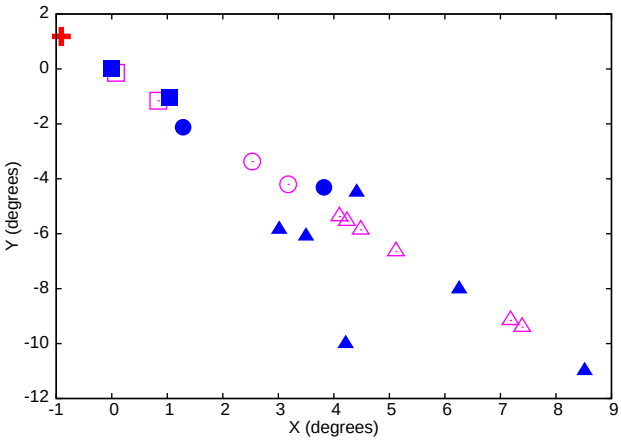

Fig. 1. Projections of the arrival directions of cosmic rays emitted by a source (cross) in the plane tangent to the celestial sphere, and centered on the highest energy event (filled square in (0,0)) emitted by the source. Deflections X and Y measured on two orthogonal axes, in degrees. Open symbols for source CR deflected by the regular GMF, only. Filled symbols for the same CR when the turbulent component is taken into account, too. Shapes correspond to CR energies (triangles: between $10^{19.0}$ and $10^{19.3}$eV, circles: between $10^{19.3}$ and $10^{19.6}$eV, squares: above $10^{19.6}$eV).

For source events, we assume power law acceleration spectra, with a power law index equal to 2.2 and a maximum energy set to 10^{21}eV. We take in most of cases a proton source and set its distance to the Earth to 50-100 Mpc. Protons are propagated to the observer by using results in ref. [14] for energy losses, which creates a "bump" in the source spectrum [15]. Then, the generated cosmic rays (CR) are deflected in the regular GMF (see e.g. [16]), and in the turbulent GMF (For more details on turbulent GMF deflections, see refs. [1] and [17]). The effects of both components are shown on Fig. 1: the regular component deflects the CR along a curve and the turbulent one spreads them "randomly" around it in a sector-shaped region. When there are many

events with same energies, they are not spread uniformly, as discussed in refs. [16], [17], [18].
Formally, results would depend on many parameters of the model and on the considered location in the sky. However in reality, there are only two essential parameters: the local deflection powers -see ref. [1]- of the regular GMF (denoted D) and of the turbulent GMF. Background events are simulated according to the energy spectrum measured by AUGER [4] and to its exposure [19].

II. METHOD

The following work is done on sky maps which only display events with energies bigger than a given threshold, E_{th}. The idea is to look for tails of lower energy events around at least two nearby events of energies $E > 10^{19.8}$eV.
We start by taking a circle around an event with $E_1 > 10^{19.8}$eV. Its radius, R, can be optimized and the value we take depends on E_{th}, D, and other parameters. R is what we can call an "internal" parameter of the method. The tail of lower energy events is searched by assuming that all events from the source are located in a sub-region of the circle, that has a sector shape with a central axis given by the second highest energy event with an energy $E_2 \leq E_1$, above a given threshold $E_2 \geq E_{2min}$, and a distance to the highest energy event compatible with an emission by the same source. This distance should be lower than β D/E_2 - D/E_1, where β is another internal parameter, and D is the assumed initial value of the local deflection power. Fig. 2 shows the probability to detect the source and the probability to be confused by background for different values of E_{2min}. We can see that one has to require $E_{2min} = 10^{19.8}$eV, in order not to detect background more frequently than source. That is why we search for at least two nearby events at the highest energies.

Then, as discriminator of source on top of background, we use a correlation coefficient -see [20]. One takes the energies E and the coordinates X' of the points located in the sector, where X' is the axis containing the first event and the center of mass of the considered points. Each point is tested and if removing them increases the correlation coefficient C(1/E,X'), then, they are definitely removed. Otherwise, they are definitely kept. If C(1/E,X') is finally bigger than a given value, C_{min}, there is detection: detection of the source in case of an initial source doublet or confusion by the background in case of an initial background doublet.
Ref. [1] discusses about optimization of the internal parameters.
In case of detection of the source, we finally reconstruct its position on the X' axis, by taking the remaining points and fitting 1/E versus X' with a straight line. This also gives an estimate of the local regular deflection power, D.

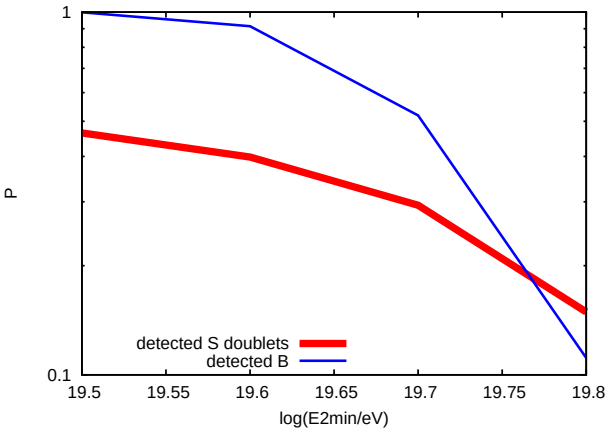

Fig. 2. Dependance on E_{2min}, the minimum energy for the second highest energy event. Thick solid line for the probability to detect the source. Thin solid line for the probability to detect background. Results presented for a source of luminosity above $10^{19.8}$eV equal to 2.6%, $E_{th} = 10^{19.3}$eV, 5000 events above 10^{19}eV in whole sky, $B_{reg} = 2\mu$G and $B_{turb} = 4\mu$G.

III. STUDY OF THE PARAMETER SPACE

We study below how the efficiency of the method presented above changes with values of physical or experimental parameters.
There are two requirements for source detection. First, the probability to detect the source doublets has to be big enough, in order not to remove too much signal. Secondly, the probability to be confused by background has to be low enough compared to the detected signal.
We define here a "cluster" as a group of at least three nearby events with very high energies: $E > 10^{19.8}$eV. The probability to have a cluster of background events is very low in case of reasonable statistics and no -or low- anisotropy: for example it is $\sim$ 1%, with 5000 events in the whole sky above 10^{19}eV and no anisotropy. However, in most of the cases, the probability to have a background doublet of very high energy events is not negligible compared to the probability to have a source doublet. That is why we separe the two cases -doublet or cluster- below. In case of a doublet, we apply the method depicted in the previous section, whereas in case of a cluster, we do not need it since the source is then already seen in $\sim$ 99% of cases. Applying the method reduces the background more than the signal from the source, but its side-effect is reducing the signal from the source in any case: that is why it is not worth applying it when the probability to be confused by background is already very low. However, when statistics increase or in case of high anisotropies above 6×10^{19}eV, background clusters become more frequent and then the method would be interesting for clusters of 3 events, too.

The figures 3 and 4 show dependance on the regular and turbulent GMF strengths. Fig. 3 is done for different values of B_{reg}, between 1 and 3 μG, with a constant ratio between regular and turbulent fields strengths. For Fig. 4, $B_{reg} = 2\mu$G and the turbulent field strength, B_{turb},

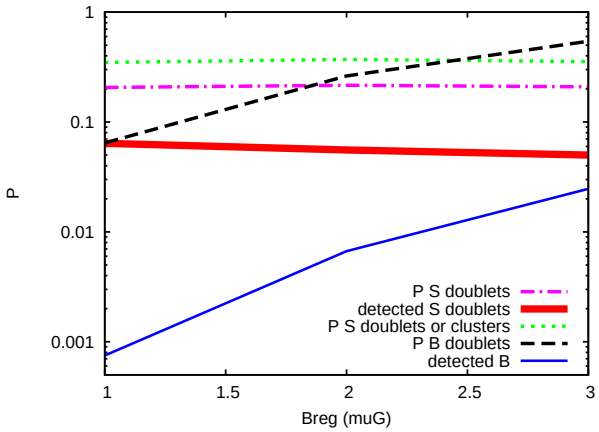

Fig. 3. Dependance on regular GMF strength, with constant ratio "regular/turbulent" set to 0.5. E_{th} = $10^{19.6}$eV. Source luminosity and number of events in the sky as for Fig. 2. Dotted line for the probability to have a doublet or a cluster from the source. Dashed-dotted and dashed lines for the probabilities to have a source or background doublet, respectively. Same line thicknesses for solid lines as for Fig. 2.

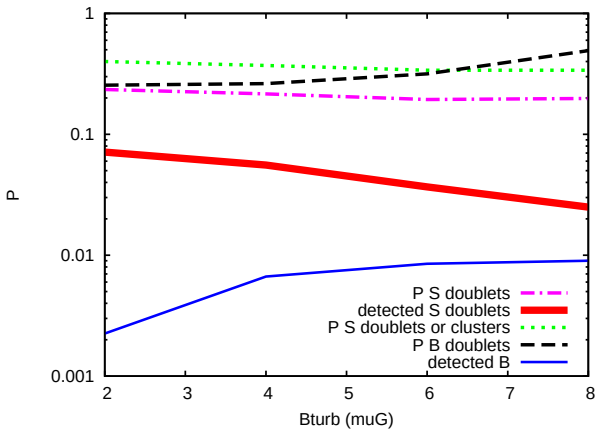

Fig. 4. Dependance on turbulent GMF strength, B_{turb}, with constant regular field set to B_{reg} = 2μG. Same values for other parameters and same line types as for Fig. 3.

varies between 2 and 8 μG. The internal parameters of the method have been roughly optimized for each different field value. The dotted line is the probability that a proton source of 2.6% luminosity above $10^{19.8}$eV emits a doublet or a cluster of events with energies E $> 10^{19.8}$eV. The dashed-dotted and the dashed lines are the probabilities to have a source or background doublet, respectively. The thick and the thin solid lines represent the probabilities to detect the source and the background, respectively. One can notice that even for the highest field values in these ranges, the ability of the method to detect the source is still quite "acceptable". The difference between the dashed and thin solid lines shows the efficiency to remove background. The difference between the dashed-dotted and thick solid lines is smaller: the signal is less removed. The difference between dotted and dashed-dotted lines is for cases when the source is already detected.

These results are computed for an isotropic sky, even at the highest energies. We checked that for reasonable values of anisotropies (if all events with energies above $10^{19.8}$eV are located in a fraction of the sky between 25% and 100%), results would be affected in a linear way. For example, in the case of 25%, the probabilities to have a background doublet and to detect it would be approximately multiplied by 4.

We have studied the dependance of source detection on source parameters. We give in [1] some numerical values for dependance on source luminosity. We also show that for example, with a regular GMF deflection power close to 5° $\times$ $10^{19.6}$eV for protons, one can still detect a light nuclei source, but only by looking for clusters if the luminosity is sufficient. In this case, the ratio "signal/background" for doublets would be too small to detect such source.

We have also worked on the dependance on experimental statistics. There is no clear and no general best energy threshold, E_{th}, to look for lower energy tails. When E_{th} is decreased, the probability to detect a source doublet through the method increases, but the probability to be confused by a background doublet increases with a bigger rate. For the example considered in [1], E_{th} = $10^{19.6}$eV $\simeq$ 4 $\times$ 10^{19}eV could be a good compromise between sufficient source detection and sufficient background rejection. The impact of total amount of experimental data mostly affects the way the detection should be done, depending on source luminosity. For example, with a bright source and high statistics like 10^4 events above 10^{19}eV, clusters appear more often and looking for them becomes a more efficient way to track the source than applying the method for doublets. However in the future, when the amount of data increases, the method used earlier for doublets can be applied to clusters, too.

IV. Reconstruction of the source position and of the regular GMF deflection power

In this section, we discuss about the ability of the method to reconstruct the source position and D.

With the assumptions considered in this paper and B_{turb} = 4μG, the source position can be reconstructed with accuracy of 1 degree in about 68% of cases for a source located in a region where D $\sim$ 5° $\times$ $10^{19.6}$eV (distribution with thick solid line on Fig. 5). Thus, resolution of the method for source position is of the order of experimental angular resolution.

Another noticeable result is that, in the same conditions, the local deflection power of the GMF regular component can be reconstructed up to 25% precision in 68% of cases, as shown on Fig. 6 (thick solid line).

Results above are mainly spoiled by the turbulent field. For comparison, we put on the same plots the distributions with B_{turb} = 0μG (thin solid line) and B_{turb} = 2μG (dashed line). The lower the turbulent field is, the better are the precisions on both results. For these lower values, the distance between reconstructed and real sources would be mostly affected by the experimental angular

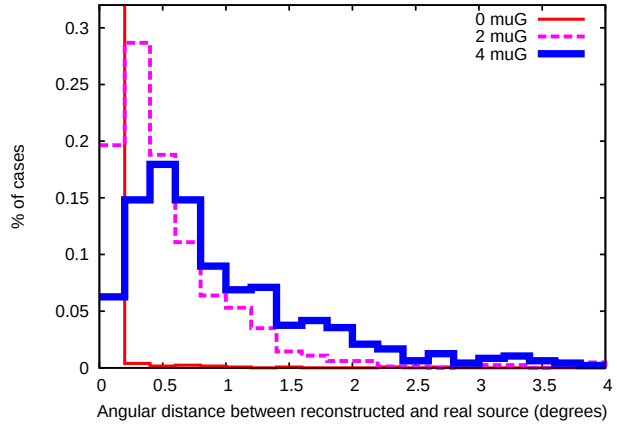

Fig. 5. Distribution of distances, in degrees, between reconstructed and real sources. Source located in a region where D $\sim 5^\circ \times 10^{19.6}$eV. Thin solid line for turbulent component off (0μG), dashed line for B_{turb} = 2μG, and thick solid line for B_{turb} = 4μG.

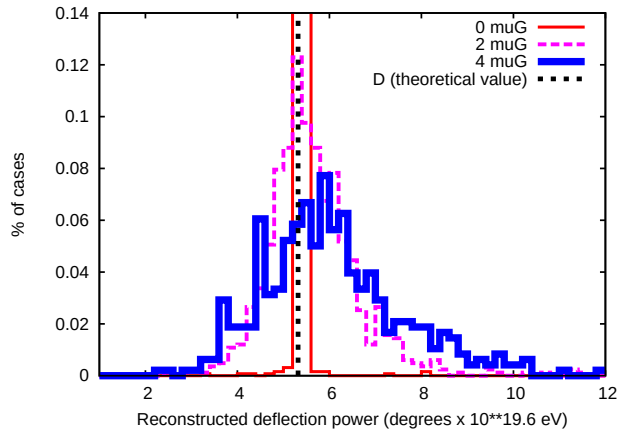

Fig. 6. Distribution of reconstructed deflection power in $^\circ \times 10^{19.6}$eV. Same parameters and line types as Fig. 5.

resolution and not by the method.

The impact of the regular field (between 1 and 3μG close to the Sun) does not change the precision on the reconstruction of D, but the precision on the source position reconstruction is better for low B_{reg} values.

If we simulate the experimental resolution on energies by taking usual values like ΔE/E = 25% instead of ΔE/E = 0 (theoretical energies), no noticeable change can be seen on our results.

V. Conclusion

We have given and studied here an alternative way to detect individual bright UHECR sources, if the deflections of UHECR due to the turbulent GMF are not too large compared to the deflections due to the regular component. We generated two sets of events: events from a source with a $1/E^{2.2}$ injection spectrum that we propagated from the source to the Earth, and events from background generated according to AUGER spectrum and exposure. We mixed them, tried to detect the source and also checked how often we got confused by background.

We showed that one should look for doublets of events with E $> 10^{19.8}$eV, when using the depicted method.

We studied in section III the dependance on several parameters: unknown parameters from the magnetic fields, the source, the sky anisotropy at high energies and statistics.

We showed in section IV that, with the parameters and assumptions adopted here, reconstruction of the source would be dominated by the current experimental angular resolution in 68% of cases and that the local deflection power can be known up to 25% in 68% of cases.

In the future, this method can be applied to experimental data to find bright UHECR sources.

References

[1] G. Giacinti, X. Derkx, D. V. Semikoz, Search for single sources of ultra-high energy cosmic rays on the sky. To be submitted to JCAP.

[2] K. Greisen, Phys. Rev. Lett. **16**, 748 (1966); G. T. Zatsepin and V. A. Kuzmin, JETP Lett. **4**, 78 (1966) [Pisma Zh. Eksp. Teor. Fiz. **4**, 114 (1966)].

[3] R. Abbasi *et al.* [HiRes Collaboration], Phys. Rev. Lett. **100**, 101101 (2008) [arXiv:astro-ph/0703099].

[4] J. Abraham *et al.* [Pierre Auger Collaboration], Phys. Rev. Lett. **101**, 061101 (2008) [arXiv:0806.4302 [astro-ph]].

[5] A. M. Hillas, Ann. Rev. Astron. Astrophys. **22**, 425 (1984).

[6] K. Ptitsyna and S. Troitsky, "Physical conditions in potential sources of ultra-high-energy cosmic rays. I. Updated Hillas plot and radiation-loss constraints," arXiv:0808.0367 [astro-ph].

[7] A. Neronov, D. Semikoz and I. Tkachev, "Ultra-High Energy Cosmic Ray production in the polar cap regions of black hole magnetospheres," arXiv:0712.1737 [astro-ph].

[8] K. Dolag, D. Grasso, V. Springel and I. Tkachev, JCAP **0501**, 009 (2005) [arXiv:astro-ph/0410419].

[9] G. Sigl, F. Miniati and T. A. Ensslin, Phys. Rev. D **70**, 043007 (2004) [arXiv:astro-ph/0401084].

[10] M. Kachelriess, P. D. Serpico and M. Teshima, Astropart. Phys. **26** (2006) 378 [arXiv:astro-ph/0510444].

[11] M. Prouza and R. Smida, Astron. Astrophys. **410** (2003) 1 [arXiv:astro-ph/0307165].

[12] A. Waelkens, T. Jaffe, M. Reinecke, F. S. Kitaura and T. A. Ensslin, "Simulating polarized Galactic synchrotron emission at all frequencies, the Hammurabi code," arXiv:0807.2262 [astro-ph].

[13] X. H. Sun, W. Reich, A. Waelkens and T. Enslin, "Radio observational constraints on Galactic 3D-emission models," arXiv:0711.1572 [astro-ph].

[14] M. Kachelriess, E. Parizot and D. V. Semikoz, "Constraining the cosmic ray source spectrum from observations in the GZK regime," arXiv:0711.3635 [astro-ph].

[15] V. S. Berezinsky and S. I. Grigor'eva, Astron. Astrophys. **199** (1988) 1.

[16] D. Harari, S. Mollerach and E. Roulet, JHEP **0207** (2002) 006 [arXiv:astro-ph/0205484].

[17] D. Harari, S. Mollerach, E. Roulet and F. Sanchez, JHEP **0203** (2002) 045 [arXiv:astro-ph/0202362].

[18] G. Golup, D. Harari, S. Mollerach and E. Roulet, AIP Conf. Proc. **1123**, 240 (2009) [arXiv:0902.1742 [astro-ph.HE]].

[19] P. Sommers, Astropart. Phys. **14** (2001) 271 [arXiv:astro-ph/0004016].

[20] D. Harari, S. Mollerach, E. Roulet and G. Golup, Detection of deflection-energy correlations with the Minimal Spanning Tree, Pierre Auger Observatory preprint GAP-2006-106